Structural Safety 97 (2022) 102211

Contents lists available at ScienceDirect

Structural Safety

journal homepage: www.elsevier.com/locate/strusafe

System-based reliability analysis of stainless steel frames subjected to gravity and wind loads

Itsaso Arrayago [a,*], Kim J.R. Rasmussen [b], Hao Zhang [b]

[a] Universitat Politècnica de Catalunya, Dept. of Civil and Environmental Engineering, Spain
[b] The University of Sydney, School of Civil Engineering, Australia

ARTICLE INFO

Keywords:
Advanced analysis
Probability-based design
Reliability calibrations
Stainless steel structures
Structural reliability
Wind loads

ABSTRACT

In the process of developing the next generation of design standards for steel structures, most relevant international structural codes including AISC 360, AISC 370, AS/NZS 4100 and Eurocode 3 already incorporate preliminary versions of system-based *design-by-analysis* approaches that allow a direct evaluation of the strength of steel and stainless steel structures from advanced numerical simulations. As a result, recent research works have focused on building rigorous structural reliability frameworks to investigate acceptable target reliability indices for structural systems and to develop new design methods in conjunction with adequate system safety factors and system resistance factors. Although design recommendations exist for the direct design of hot-rolled and cold-formed steel structures based on advanced finite element analysis, the extension of the method to other materials such as stainless steel is under development. This paper is part of a research effort to build a reliability framework for stainless steel structures subject to different load combinations and presents the results of system reliability calibrations carried out on six stainless steel portal frames subjected to combined gravity and wind loads. The study covers the most common stainless steel families and three international design frameworks (i.e., Eurocode, US and Australian frameworks). From the reliability calibrations derived, suitable system safety factors $\gamma_{M,s}$ and system resistance factors ϕ_s are proposed for the direct design of stainless steel frames under combined gravity and wind loads using advanced numerical simulations.

1. Introduction

As a consequence of the rapid advances in design software and the growth of computational features of desktop computers over the last decade, the behaviour and failure of complex structural systems can be accurately predicted. In response to these advances, current research efforts are focused on the development of direct *design-by-analysis* approaches, in which the analysis and design are carried out simultaneously (*single-step* process) by accounting for all geometric and material nonlinearities in the analysis and without the use of analytical design expressions. Direct design approaches can be applied to members (e.g., beam-columns), parts of structures (e.g., a module of a box-girder comprising the deck of a bridge) or systems (e.g., full frames). In this process, most relevant design codes for steel and stainless steel structures in the Australian, US and Eurocode frameworks (AS/NZS 4100 [1], AISC 360-16 [2], AISC 370-21 [3], prEN 1993-1-14 [4]) already incorporate preliminary versions of direct design methods, although current design provisions are still primarily based on the conventional *two-step* approaches [1-3,5-8]. In the *two-step* limit state approach, designers are required to determine internal actions from a usually elastic structural analysis and to subsequently check the ultimate capacity of the different members and connections comprising the structural system. Alternatively, when designing (or verifying) with direct methods the strength of a member or a structure can be directly evaluated from advanced simulations without requiring further checks; when applied to systems, the load redistribution capacity, redundancy and robustness of the structures can be fully exploited, ensuring a more uniform reliability across different structural systems and potentially leading to lighter and more economical designs [9].

In the traditional *two-step* approach, the random variations of design parameters are dealt with nominal or characteristic values and the use of the partial coefficients, and the capacity of structures is generally limited to the resistance of individual members or connections, which are evaluated from time-consuming and often complex design expressions. Conversely, direct design procedures are simple, as shown in Eq. (1) and Eq. (2) for the Eurocode and the US/Australian design

* Corresponding author at: Jordi Girona 1-3, Building C1, 08034 Barcelona, Spain.
E-mail address: itsaso.arrayago@upc.edu (I. Arrayago).

https://doi.org/10.1016/j.strusafe.2022.102211
Received 4 January 2021; Received in revised form 22 February 2022; Accepted 24 February 2022
Available online 28 March 2022

frameworks, respectively, where R_k (or R_n) is the characteristic (or nominal) resistance of the system, γ_i is the load magnification factor, Q_{ki} (or Q_{ni}) denotes the characteristic (or nominal) structural loads, and $\gamma_{M,s}$ (or ϕ_s) is the partial safety factor (or resistance factor) of the system.

$$\frac{R_k}{\gamma_{M,s}} \geq \sum \gamma_i Q_{ki} \tag{1}$$

$$\phi_s R_n \geq \sum \gamma_i Q_{ni} \tag{2}$$

When nonlinear structural analyses are carried out, design loads are generally applied proportionally and incrementally by using a load scale factor λ. The ultimate load scale factor λ_u (when the frame is at the state of incipient collapse) is referred to as the resistance of the frame. In such cases, Eq. (1) and Eq. (2) can be rewritten as Eq. (3) and Eq. (4), respectively. Obviously, the ultimate load scale factor corresponds to a particular load pattern, and consequently, the statistics of λ_u (and the corresponding $\gamma_{M,s}$ and ϕ_s factors) may depend on the loading pattern. The present study assumes some representative loading patterns and different loading scenarios for stainless steel portal frames, and it is expected that these will cover the typical design situations.

$$\lambda_u \geq \gamma_{M,s} \tag{3}$$

$$\lambda_u \geq \frac{1}{\phi_s} \tag{4}$$

Despite including direct design approaches, current design standards [1-4] do not provide system-based safety factors (or resistance factors). Rather, they require a comparable or higher level of reliability than that achieved for existing member-based provisions without stating how this may be demonstrated. Hence, it is necessary to determine suitable system safety factors $\gamma_{M,s}$ or system resistance factors ϕ_s from rigorous structural reliability considerations for different structural types and materials to be adopted in system-based direct design approaches. Based on recent research works over the last years, design recommendations have been proposed for the design of hot-rolled steel frames [9-12], cold-formed steel frames [13,14], steel storage rack frames [15] and steel scaffolds [16] using system-based direct design approaches. However, the extension of the recommendations to different materials such as stainless steel requires independent reliability calibrations due to the noticeable nonlinear stress–strain response and significant strain-hardening properties exhibited by these materials [17-19]. This is being addressed in the NewGeneSS project [20]. To date, system safety factors $\gamma_{M,s}$ and system resistance factors ϕ_s have been derived for stainless steel frames under gravity loads [21], based on the statistical characterization of the different random variables affecting the strength of stainless steel structures reported in [22].

This paper presents the extension of the system-based direct design approach to stainless steel cold-formed portal frames subjected to combined gravity and wind loads through the calibration of suitable system safety factors $\gamma_{M,s}$ and resistance factors ϕ_s. A brief description of the baseline frames and the developed Finite Element models is given in Section 2, while the load pattern adopted and the failure modes of the frames are described in Section 3. Section 4 builds the full reliability analysis framework for stainless steel frames, including the probabilistic models considered for the different random variables and the methodology adopted for the calibration of system reliabilities. Finally, Section 5 presents and compares the results of the reliability calibrations for the different design frameworks investigated, proposes suitable system safety factors $\gamma_{M,s}$ and resistance factors ϕ_s for the Eurocode, US and Australian frameworks, compares the baseline frames with those designed using the traditional *two-step* approach and provides recommendations for specification committees.

2. Finite element modelling

2.1. Description of baseline frames

The system-based reliability calibrations presented in this paper are based on the results of six single-storey, single-bay stainless steel portal frames of the type shown in Fig. 1, featuring the typical austenitic stainless steel grade EN 1.4301 (ASTM 304) for Frames 1 and 2, the common EN 1.4462 (ASTM 2205) duplex stainless steel grade for Frames 3 and 4, and the basic ferritic grade EN 1.4003 (ASTM UNS S40977) for Frames 5 and 6. These six baseline frames are identical to those adopted in [21] for the reliability analysis of stainless steel frames under gravity loads, with the overall frame geometries (span length s, heights at the eaves H_1 and at the roof ridge H_2) summarized in Table 1. All frames comprised cold-formed rectangular hollow section (RHS) members, with uniform section geometries for all rafters and columns. Frames 1, 3 and 5 featured the compact 150×100×4 cross-section and Frames 2, 4 and 6 were made from the slender 250×150×4 cross-section, where the H×B×t notation indicates the cross-section height H, width B and thickness t. Note that Frames 1, 3 and 5 had the same overall and cross-sectional dimensions but different materials, which allowed evaluating the effect of the stainless steel family on the derived system reliabilities.

Stainless steel alloys exhibit a pronounced nonlinear stress–strain response with significant strain-hardening, which is one of their most characteristic features together with their inherent corrosion resistance [17,18]. To describe both material nonlinearity and strain-hardening, the two-stage model proposed in [23,24] and adopted in the current international design standards for stainless steel structures was used [3,4,7,25], with the basic material parameters specified in the relevant material standards [3,7,25,26]. Since the cross-sections analysed were cold-formed, the increase in resistance due to the significant plastic deformations occurring during the manufacturing process were considered through the enhanced yield stress values predicted from the model proposed in [27]. The nominal stress–strain curves for the different stainless steel alloys corresponding to the three design frameworks are shown in Fig. 2.

The stiffened welded knee connections suitable for rigid portal frames defined in [28] were adopted for the joints of the cold-formed RHS frames, since these connections provide sufficient rotation capacity for plastic hinges to develop. According to the discussion presented in [21], the moment–rotation curve of these connections can be reasonably represented by a bi-linear model defined through two stiffness parameters K_1, K_2 and two moment capacities M_1 and M_2. The nominal parameters defining the behaviour of the connections at the eaves, apexes and column bases are identical to those adopted in [21] except for the base connections in Frames 2, 4 and 6, which featured pin-ended base support conditions under gravity loads only, and are reported in Table 1.

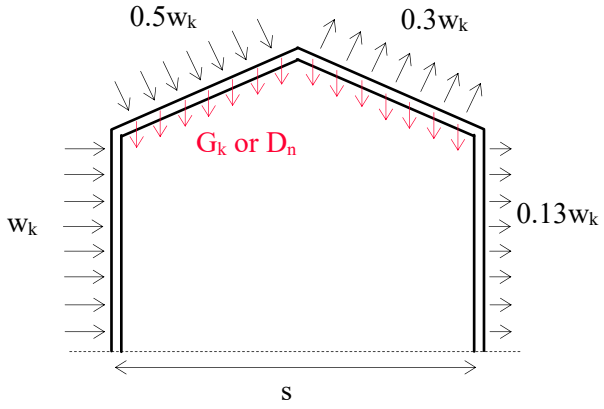

Fig. 1. Gravity and wind load patterns (adapted from [21]).

Table 1
Key parameter definition of nominal frames (adapted from [21]).

Variable group	Variable	Austenitic stainless steel		Duplex stainless steel		Ferritic stainless steel	
		Frame 1	Frame 2	Frame 3	Frame 4	Frame 5	Frame 6
Overall frame geometry	s [m]	8.0	10.0	8.0	12.0	8.0	11.0
	H_1 [m]	4.8	6.4	4.8	6.6	4.8	6.5
	H_2 [m]	6.0	7.0	6.0	7.4	6.0	7.2
Joint behaviour at bases	$K_{1,base}$ [kNm/rad]	4000	5000	4000	5000	4000	5000
	$K_{2,base}$ [kNm/rad]	400	500	400	500	400	500
	$M_{1,base}$ [kNm]	26.3	52.3	41.4	90.3	27.0	53.9
	$M_{2,base}$ [kNm]	40.4	80.2	63.4	109.5	41.4	82.6
Joint behaviour at eaves	$K_{1,eave}$ [kNm/rad]	6400	7000	6400	9000	6400	8000
	$K_{2,eave}$ [kNm/rad]	640	700	640	900	640	800
	$M_{1,eave}$ [kNm]	23.9	50.0	37.6	86.4	24.6	51.5
	$M_{2,eave}$ [kNm]	37.4	78.2	58.7	105.4	38.4	80.5
Joint behaviour at apex	$K_{1,apex}$ [kNm/rad]	6600	7500	6600	9500	6600	8500
	$K_{2,apex}$ [kNm/rad]	660	750	660	950	660	850
	$M_{1,apex}$ [kNm]	25.4	53.1	39.9	91.8	26.1	54.8
	$M_{2,apex}$ [kNm]	37.4	78.2	58.7	105.4	38.4	80.5
Level of dead load	GW1 - G_k or D_n [kN/m]	1.00	1.40	2.00	2.00	1.00	1.60
	GW2 - G_k or D_n [kN/m]	0.75	1.20	1.50	1.60	0.75	1.40
	GW3 - G_k or D_n [kN/m]	0.60	1.00	1.00	1.40	0.60	1.20

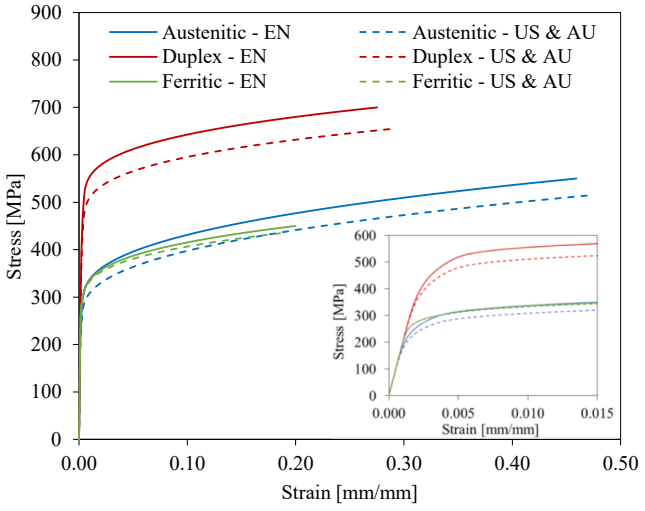

Fig. 2. Nominal stress–strain curves for the different stainless steel alloys and design frameworks considered.

Note that this study does not consider joint failure; it assumes that the joints possess sufficient strength and ductility for their failure (e.g., brittle failure) not to occur prior to reaching the ultimate limit states of the frames. This assumption is, however, only valid for the calibration of system safety and resistance factors carried out in this paper. In practical design, and while the existing direct design recommendations do not feature joint failure, engineers should verify that the connections do not fail under the predicted frame capacities using current design specifications, and demonstrate that they possess sufficient strength and ductility for the frame ultimate limit states to be reached.

2.2. Description of finite element models

System strengths of cold-formed stainless steel frames were estimated from advanced finite element (FE) simulations using the general-purpose software ABAQUS [29]. The FE model used to simulate the behaviour of stainless steel frames under combined gravity and wind loads was identical to that used in [21] for gravity load cases, to which only small changes were made to introduce the wind loads. The full details of the finite element models are described and discussed in [21] and only the key aspects are summarized in this Section. The frames were modelled using S4R shell elements [21,30-32], with a mesh size of approximately 25 mm × 25 mm as per the mesh convergence study reported in [21]. The finite element models developed included local, member out-of-straightness and frame out-of-plumbness initial geometric imperfections, with appropriate shapes and amplitudes: while the requirements in [1-4,6,33] were followed for the imperfections in nominal frames, the values determined from the statistical distributions discussed in Section 4.1 were adopted for the structural analysis models. The full discussion on the initial imperfections considered by the different design frameworks can be found in [21]. These imperfections were input in the FE models following different strategies: while local and member imperfections were introduced from prior linear buckling analyses, global imperfections were directly defined by offsetting the position of the nodes.

This study assumed bending residual stresses following the model proposed in [34] for cold-formed stainless steel rectangular hollow sections, which were introduced as initial stresses in the FE models, and membrane residual stresses were neglected. Likewise, material properties were assigned to the different models through user-defined true stress *vs* true plastic strain relationships, assuming a von Mises yield surface with isotropic hardening [35] and the associated flow rule available in ABAQUS [29]. The frame models comprised four independent columns and rafters, which were connected to each other through the combination of kinematic couplings, reference points and *HINGE, BEAM* and *UJOINT* connector elements described in [21], to which user-defined bi-linear moment–rotation curves were specified. To limit the response of the frames to the in-plane behaviour, the out-of-plane displacements of the nodes defining the apex and eaves joint points, and the mid-height sections of the columns and the mid-length sections of the rafters were restrained.

The ultimate frame loads were determined from static pushover analyses in which dead loads were first applied at the upper faces of the rafters as *TRVEC* surface traction loads, followed by the wind loading pattern shown in Fig. 1 until the collapse of the frames was reached. Wind loads were introduced as *PRESSURE* loads using the appropriate magnitude and sign in each column and rafter. While the geometrically and materially nonlinear analyses corresponding to the dead loading increments were performed using the Static General method, the Static Riks method was adopted for the analysis of wind loading increments [29].

2.3. Validation of finite element models

The validation of the developed finite element models was carried out by comparing the experimental results of the stainless steel frame

tests reported in [32,36] with the corresponding simulation results obtained from the FE model described in Section 2.2. The experimental specimens corresponded to four single-span, single-storey cold-formed RHS austenitic stainless steel frames featuring compact and slender sections, and were subjected to vertical and horizontal loading. The FE models used in the validation were built as discussed in the previous Section, but included some specific features measured from the experimental specimens and reported in [32,36], including loading sequence and the position of the loads, material properties (obtained from tensile coupon tests), the rotational stiffness values at the connections (estimated from experimental results at the base and eaves joints), and initial imperfection amplitudes (measured from the specimens). Details of the model validation, the results in terms of numerical-to-experimental load ratios and displacement ratios, and the comparison between experimental and numerical load–displacement curves can be found in [21], which indicated that the developed FE models were capable of accurately replicating the behaviour of the frames under combined vertical and horizontal loading. It should be noted that although the actual properties measured from the specimens were adopted in the simulations reproducing the tests for the validation of the FE model, random properties based on the stochastic models discussed in Section 4.1 were assumed for the simulations considered in reliability calibrations.

3. Stainless steel frames under gravity and wind loads

3.1. Gravity and wind loading

The reliability calibrations for stainless steel frames subjected to wind loads were based on a loading pattern that combines both gravity and wind loads, as shown in Fig. 1. The ultimate limit states of the frames were determined from static pushover analyses in which dead loads G_k or D_n were firstly applied to the rafters in full, followed by the incremental application of wind loading until the lateral resistance of the frames was reached (i.e., the frame was "pushed" over). To investigate the effect of the wind-to-dead load ratio in reliability calibrations, three different values of design (nominal) dead loads G_k (or D_n) were considered for each frame, namely the GW1, GW2 and GW3 load scenarios, representing relatively light, medium and heavy wind loads, as reported in Table 1.

Nominal wind load patterns and magnitudes are prescribed in the different wind loading standards for the Eurocode, US and Australian design frameworks, prEN 1991-1-4 [37], ASCE 7-16 [38] and AS/NZS 1170.2 [39], respectively. The characteristic value of the wind load for the Eurocode framework is given by Eq. (5), in which c_e is the exposure factor accounting for the effect of height and terrain roughness, c_p is the pressure coefficient, c_s is the size factor, c_d is the dynamic amplification factor and q_{ref} is the peak velocity pressure, which is dependent on the square of the wind speed.

$$W_k = c_e \cdot c_p \cdot c_s \cdot c_d \cdot q_{ref} \tag{5}$$

Alternatively, the general form of the wind load acting on a structure according to the ASCE 7-16 [38] Specification is given in Eq. (6), where C is a constant, G is the gust factor, C_p is the pressure coefficient, K_z is the exposure factor, K_d is the directionality coefficient and V_{max} is the wind speed. The wind load corresponding to the Australian framework given in AS/NZS 1170.2 [39] can be generally written as per in Eq. (7), in which c is a constant, C_{fig} and C_{dyn} are the aerodynamic shape factor and the dynamic response factor, respectively, and $V_{des,\theta}$ is the orthogonal design wind speed, which depends on the wind speed, the terrain, the shielding and the topography.

$$W = C \cdot G \cdot C_p \cdot K_z \cdot K_d \cdot V_{max}^2 \tag{6}$$

$$W = c \cdot C_{fig} \cdot C_{dyn} \cdot V_{des,\theta}^2 \tag{7}$$

From these wind load models, it is evident that, despite featuring several modifying coefficients, the three models include a part that is a function of the square of the wind speed and different time-invariant factors related to the roughness, exposure and dynamic effects that depend on the characteristics of the site and the interaction between the structure and the wind. The three wind load models prescribed in the different specifications present different definitions for the wind field characteristics and the magnitudes of the nominal wind loads depend on several factors, the most relevant of which are the averaging times for basic wind velocity (ASCE 7-16 [38] and AS/NZS 1170.2 [39] define the basic wind speed as 3-s gust speed whereas prEN 1991-1-4 [37] defines it as the 10-min mean wind speed), the wind velocity profiles (AS/NZS 1170.2 and prEN 1991-1-4 use logarithmic laws, while ASCE 7 uses a power law) and the internal and external pressure coefficients (which determine the wind loading patterns and essentially depend on the geometry of the frame – pitch angle, number of openings – and the direction of the wind), inevitably presenting some variability in the final wind loads. However, a study comparing international wind load specifications found that, although significant discrepancies exist for the intermediate parameters, the different models result in reasonably consistent overall loads when the basic wind velocity is modified to match the velocity pressure and the same force/pressure coefficients are assumed [40].

When defining the wind loading pattern adopted in this study, the provisions and pressure coefficients prescribed in prEN 1991-1-4 [37] were considered. Wind pressures on wall and roof elements were determined for the overall frame geometries given in Table 1 and resulted in the average external wind pressure distribution shown in Fig. 1, which is similar to the pattern adopted in a recent reliability study on steel frames carried out in the Eurocode framework [41]. Although it is based on prEN 1991-1-4 [37] provisions, this study assumed that the wind loading pattern is still applicable to the analysis of the US and Australian design frameworks since the differences in design wind loads are fundamentally governed by the design wind load magnitudes rather than by the loading patterns resulting from particular pressure coefficients. Note that this paper assumes ordinary (synoptic) winds, without considering coastal areas subjected to tropical cyclones or hurricane-prone regions.

3.2. Failure modes of baseline frames

This Section describes the failure modes observed for the six baseline nominal frames under the dead and wind loading pattern shown in Fig. 1. Nominal models were built using the FE model described in Section 2.2, the parameters reported in Table 1 and the nominal material properties specified in [3,7,25,26]. The failure modes observed for each frame in the three design frameworks investigated were essentially the same, although the values of the predicted ultimate failure wind loads were found to be slightly different, as discussed in Section 5.1.

Frames 1, 3 and 5 had relatively low heights and spans, and each frame corresponded to one of the three stainless steel families investigated, austenitic, duplex and ferritic stainless steel alloys, respectively. At the ultimate limit state, these frames exhibited considerable lateral drifts and small vertical deflections at the apex sections, as shown in Fig. 3, although the deflections observed varied remarkably for the different dead load levels considered. The cross-sections adopted for these frames comprised compact sections with low local cross-sectional slenderness values and considerable capacity to redistribute stress inelastically for the austenitic and ferritic materials considered (Frames 1 and 5). However, for the duplex stainless steel Frame 3, these same cross-section dimensions resulted in a significantly higher local slenderness owing to the higher yield stress characterizing the EN 1.4462/ ASTM 2205 duplex grade, and therefore limited the stress redistribution capacity of the frame when compared to Frames 1 and 5. Austenitic and ferritic Frames 1 and 5 failed showing spatial yielding at the critical cross-sections. At wind load levels of around 80% of the ultimate loads, spatial plastic hinges formed at the two column bases, and

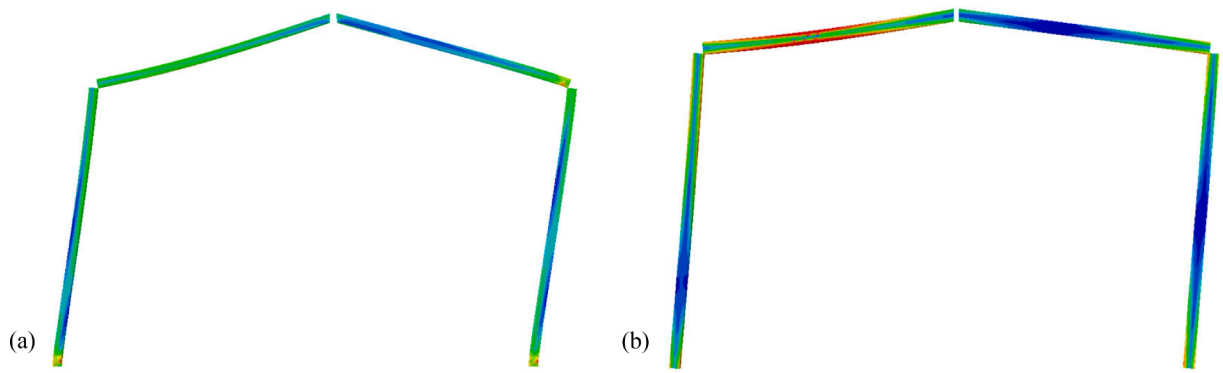

Fig. 3. Typical failure modes for (a) short and (b) long span stainless steel frames under combined gravity and wind loads.

the failure of the frames occurred soon thereafter when plastic hinges formed at the rafters near the right eaves. At the ultimate limit states, considerably high stresses of about 1.50 and 1.35 times the yield stress were observed at the column bases for Frame 1 and Frame 5, respectively, due to strain-hardening. At later stages of frame deformations, local failures were visible in the compressed areas of the columns near the base connections and at the right eave connections. On the contrary, failure of the duplex stainless steel Frame 3 occurred after the column bases reached stress levels equivalent to the enhanced yield stress at wind load values of about 90% of the ultimate loads. Although this frame was capable of withstanding marginally higher loads, it failed before any spread of yielding was observed at the right eave due to the limited redistribution capacity of the cross-section.

Frames 2, 4 and 6 exhibited relatively long spans and more slender cross-sections. These frames also showed significant lateral drifts in their ultimate states, and vertical deflections at the apex sections were larger than for the frames with shorter spans. The failure mode for Frame 4, typical for the long span frames analysed, is shown in Fig. 3. While the RHS sections corresponding to austenitic and ferritic stainless steel alloys (Frames 2 and 6) had local slenderness values close to the limit between slender and fully effective sections, the nominal cross-section in the duplex Frame 4 was a slender section under compression. Consequently, these sections were incapable of developing strain-hardening or bending moment redistribution. Failure of Frames 2, 4 and 6 occurred when the capacities of the column bases and right eaves were reached, which corresponded to stress levels similar to the corresponding nominal enhanced yield stress for Frames 2 and 6, but to considerably lower stresses for Frame 4 due to the interaction with local buckling. For each frame, the failure of the three critical sections occurred for very similar wind load levels. Due to the larger spans adopted for these frames, significant flexural deformations and stresses were observed at the central parts of the left rafters at their respective ultimate limit states, particularly for Frame 4 and Frame 6 (see Fig. 3).

4. System strength reliability calibrations

This Section presents the statistical models adopted in the reliability calibration, including the main random variables affecting the system strength of stainless steel structures, model uncertainties and loads. The Section also describes the methodology adopted in the system reliability analysis of frames subjected to combined gravity and wind loads for the three design frameworks investigated, i.e., the Eurocode, US and Australian frameworks.

4.1. Statistics of the uncertain variables affecting the strength

Defining appropriate stochastic models for system strength distributions of actual stainless steel frames subjected to combined gravity and wind loads is fundamental for the calibration of the system partial safety factors and system resistance factors. These statistical models were estimated from extensive numerical simulations accounting for the variability of different material, imperfection and geometric random characteristics affecting the strength of stainless steel frames, as well as uncertainties associated with FE simulations. The statistical models assumed for the variability of the random variables are discussed in [21], and only a brief summary is provided herein.

The stochastic models for the variability of material parameters, cross-section geometric properties, imperfections (at frame, member and local levels) and residual stresses considered in this study were specific to cold-formed stainless steel members [22] and identical to those adopted in [21]. It is important to highlight that the yield overstrength ratios (i.e., mean-to-nominal yield stress ratios) reported in [22] for cold-formed stainless steel materials are significantly high, with $\bar{f}_y/f_{y,n}$ ratios being 1.30 for austenitic and ferritic families and 1.15 for duplex alloys. Due to the limited availability of real measurements on frame imperfections for stainless steel frames, this study assumed the stochastic variability of the out-of-plumb angle ϕ adopted in [14] for cold-formed steel frames. Likewise, uncertainties associated with the behaviour of stainless steel stiffened welded connections were also defined based on the data available for steel connections [14], since the measurements to characterize the variability of the K_1, K_2, M_1 and M_2 parameters for stainless steel joints were deemed to be insufficient [21]. The last stochastic variable affecting the resistance of stainless steel frames considered in this study was model uncertainty γ_{FE} or θ, and accounted for the approximations and assumptions made when determining the strength of structural systems using advanced FE simulations. Given the reduced number of experimental results available for stainless steel frames, insufficient to derive a specific probabilistic characterization of the model uncertainties, these were accounted for through unbiased log-normal distributions with a COV of 0.05 [42,43].

Assuming that the variability of the overall frame properties was negligible in comparison with the variability of other variables included in the analysis, such as loads and material properties, this analysis and the study presented in [21] considered frame spans, column heights and heights at apex sections as deterministic variables. In addition, the parameters governing the behaviour of connections and the amplitudes and directions of member and local imperfections were considered as uncorrelated random variables, while material properties, residual stress magnitudes and cross-sectional properties were assumed to be perfectly correlated between all members. This last approach was found to be a conservative assumption for reliability evaluations in [10], where the effect of the spatial correlation of the material properties on the system reliability was investigated. The study considered perfectly-correlated, uncorrelated and partially-correlated member properties, and concluded that while the mean-to-nominal strength ratios were very similar in all cases, the COV values reduced for decreasing correlation, with an extent depending on whether serial or parallel system effects were dominant. Nevertheless, the final system resistance factors

Table 2
Statistics of loads.

Framework	Load type	Mean	COV	Statistical distribution	Reference
Eurocode framework	Dead load G	$1.00G_k$	0.10	Normal	[42]
	Wind load W_{max}	$0.72W_{k,50}$ *	0.36	Extreme Type I	–
US framework	Dead load D	$1.05D_n$	0.10	Normal	[44]
	Wind load W_{max}	$0.75W_{n,50}$ *	0.35	Extreme Type I	[45]
	Wind load W_{max}	$0.47W_{n,700}$ †	0.35	Extreme Type I	–
Australian framework	Dead load G	$1.05G_n$	0.10	Normal	[21]
	Wind load W_{max}	$0.68W_{n,50}$ *	0.39	Extreme Type I	[47]
	Wind load W_{max}	$0.45W_{n,500}$ ‡	0.39	Extreme Type I	–

* Nominal wind load is based on a return period of T = 50 years.
† Nominal wind load is based on a return period of T = 700 years.
‡ Nominal wind load is based on a return period of T = 500 years.

calibrated were found not to be affected by the degree of correlation in member properties, although this finding is dependent on the redundancy of the system.

4.2. Load statistics

The adoption of probabilistic models representing the maximum load to occur within a reference period is fundamental to evaluate system reliability. This study is based on a reference period of 50 years, which corresponds to the design service life for typical building structures and to which the stochastic models available in the literature generally correspond. Statistical models adopted in the literature for dead (or permanent) loads and wind loads in the different design frameworks investigated tend to be consistent in terms of the distribution types adopted, but show different mean-to-nominal and COV values, especially for wind loads. In general, dead loads are assumed to be normally distributed for the three design frameworks [42-44], with mean-to-nominal values equal or very close to unity and small coefficients of variation, as shown in Table 2.

Gravity loads can be governing in the design of stainless steel frames, especially imposed loads, but it is usually the wind loading that has major influence in the final solution adopted. Nominal wind loads calculated from the different wind loading standards depend on a number of parameters, as discussed in Section 3.1. All these parameters are random in nature and are usually difficult to estimate since they require extensive measurement databases to be calibrated, and consequently, they are recurringly updated as more data becomes available, modifying the wind load probabilistic models [45]. The wind load of interest in reliability analysis is the maximum wind load to occur within the reference period defined for the study (denoted by W_{max}), which in this case corresponds to 50 years. Traditionally, loading standards have specified nominal or design wind loads using the wind speeds corresponding to a return period of T = 50 years, denoted by $V_{n,50}$. Thus, the mean values of the maximum wind load W_{max} corresponding to a reference period of 50 years have been historically expressed using the nominal winds for a return period of T = 50 years, $W_{n,50}$.

Wind speeds are generally assumed to follow Extreme Type I distributions, although wind loads depend not only on the squares of wind speed, according to the models described in Section 3.1, but also on a series of additional random parameters. Thus, the derivation of the probabilistic distribution describing the wind load W_{max} is not direct. The approach followed by Ellingwood et al. [46] was to compute the cumulative probability distribution of the wind load function given in Eq. (6) numerically, assuming that each component in the wind loading chain was an independent random variable and assigning probabilistic distributions to each of them. The study used wind speed data from different sites and assumed that the gust factor G, the pressure coefficient C_p and the exposure factor K_z followed unbiased normal distributions. The distribution for the wind load was estimated through Monte Carlo simulation and fitted to the 90th percentile and above by an Extreme Type I distribution with a mean-to-nominal wind load ratio of 0.90 and a COV of 0.35. This wind load model has been systematically used in the calibration of the load factors of the different editions of the ASCE 7 Specification. However, recent studies have shown that a certain bias exists in the directionality factor, and the wind load model derived in [46] was updated to account for this bias, reducing the mean value of the wind load to $0.75W_{n,50}$ while keeping the COV constant [45], as reported in Table 2. A similar approach was adopted in [47] when deriving the statistics for the wind loads in Australia, also resulting in an Extreme Type I distribution with a mean value of the maximum wind load equal to $0.68W_{n,50}$ and a COV of 0.39.

With the aim of determining the wind load distributions in the Eurocode framework, a Monte Carlo simulation was carried out in this paper following the methodology adopted in [46], but using the $W = q_{ref} \cdot c_e \cdot c_p \cdot c_g$ wind load model and the statistics for the different wind load components reported in Table 3. Note that while the peak velocity pressure q_{ref} represents the time-variant part of the wind load model and depends on the wind climate, the rest of the factors constitute the time-invariant part of the model, which convert the wind pressure into a wind loading on the structure. Additional uncertainties have been considered through the model coefficient, as in [42]. For the time-invariant part of the model the distributions based on recent studies by Botha et al. [48,49], and reported in Table 3, were considered, which concluded that the wind load components with the greatest effect on the total wind load uncertainty are the peak velocity pressure q_{ref}, the exposure factor c_e and the pressure coefficient c_p. New probabilistic models were also developed in [48], indicating that the existing wind load models underestimate the uncertainty of these time-invariant wind load components as reduced biases and larger variabilities were observed. The probabilistic models reported in Table 3 for c_e and c_p are based on the combination of the new models derived in [48] and the original models used in [42,50] to assess the Eurocode, following the approach adopted in [49]. The final fit of the cumulative probability distribution for the wind load above the 90th percentile resulted in an Extreme Type I distribution with a mean-to-characteristic value of 0.72 and a COV value of 0.36, which is similar to the revised wind load statistics derived in [45] for the US framework and the models used for the assessment of the Eurocode in [42,51,52] (i.e., a mean value of $0.70W_{k,50}$ and a COV of 0.35).

Table 2 summarizes the statistics of the wind loads adopted for the different design frameworks. These results indicate that wind load statistics are comparable for the three different design frameworks

Table 3
Distributions of wind load components adopted in the derivation of the wind load model for the Eurocode framework.

Variable	Mean	COV	Statistical distribution	Reference
Basic wind pressure, q_{ref}	1.10	0.18	Extreme Type I	[42]
Roughness factor, c_e	0.84	0.12	Normal	[48]
Pressure coefficient, c_p	1.00	0.16	Normal	[48]
Gust factor, c_g	1.00	0.10	Normal	[42]
Model coefficient	0.80	0.20	Normal	[42]

considered. It shall be noted that the current versions of the US and Australian wind loading standards define the nominal wind speeds using significantly higher return periods (i.e., 700 or 500 years). In contrast, wind actions calculated using prEN 1991-1-4 [37] are intended to be characteristic values corresponding to annual exceedance probabilities of 2%, which are closely equivalent to a return period of 50 years. The adoption of higher return periods in ASCE 7-16 [38] and AS/NZS 1170.2 [39] allowed for the "cyclone factors" to be eliminated in the new standards, but required a re-calibration of the models describing the statistics of W_{max} wind loads for these frameworks. For this, the approximate relationship between the nominal wind loads for a T-year return period W_T and the wind load for a 50-year return period W_{50} proposed in [45], and given by Eq. (8), can be used, which is valid for most of the non-hurricane-prone regions of the US (ASCE 7 [38]).

$$W_T = W_{50}[0.36 + 0.10 \cdot \ln(12T)]^2 \quad (8)$$

Nominal wind loads codified in the ASCE 7-16 [38] Specification for Risk Category II structures correspond to a return period of T = 700 years, while the AS/NZS 1170.2 [39] Specification features design wind speeds for a return period of 500 years for Importance Level 2 structures and 50-year service lives. Using Eq. (8), the relationships between $W_{n,50}$ and $W_{n,700}$ and $W_{n,500}$ can be evaluated, and from these the means of W_{max} relative to the $W_{n,700}$ and $W_{n,500}$ nominal loads can be estimated using the mean-to-$W_{n,50}$ values reported in Table 2. For the ASCE 7-16 [38] Specification, $W_{n,700}/W_{n,50} = 1.60$ is obtained from Eq. (8), which results in a mean of W_{max} equal to $0.75W_{n,50} = 0.75W_{n,700}/1.60 = 0.47W_{n,700}$. Although the W_T/W_{50} ratio depends on the local wind climate and Eq. (8) is valid for non-hurricane-prone regions of the US, in the absence of an equivalent expression for the extratropical regions in Australia the same relationship has been adopted to estimate the $W_{n,500}/W_{n,50}$ ratio. Hence, for the AS/NZS 1170.2 [39] Specification with a nominal wind load corresponding to a 500-years return period, $W_{n,500}/W_{n,50} = 1.51$ is obtained and the mean of W_{max} is recalculated as $0.68W_{n,50} = 0.68W_{n,500}/1.51 = 0.45W_{n,500}$. It is worth noting that the wind loads have remarkably similar statistics in the current ASCE 7-16 [38] and AS/NZS 1170.2 [39] specifications, with mean values of the maximum wind load W_{max} around $0.45W_n - 0.47W_n$ and coefficients of variation of 0.35−0.39. In summary, while the wind load distributions adopted in this study for the US and Australian frameworks corresponded to these mean and COV values, a mean of the maximum wind load W_{max} and COV equal to $0.72W_{k,50}$ and 0.36, corresponding to a 50-years return period, were considered for the Eurocode framework; all wind loads were modelled as Extreme Type I largest distributions.

4.3. System reliability analysis method

The failure of a structural system is usually quantified by its probability of failure P_f, which is traditionally measured through the reliability index β. The probability of failure P_f is related to the reliability index by $\beta = \Phi^{-1}(1 - P_f)$, where Φ^{-1} is the inverse standard normal distribution function [53,54]. Although Direct Monte Carlo simulation is often used as a method of evaluating structural reliability, it can be computationally too demanding in studies where nonlinear shell-element based simulations are performed. For this reason, the study presented in this paper was based on the simplified yet robust reliability analysis method introduced in [10,14]. This method relies on the characterization of the stochastic properties of the resistance of frames using random sampling techniques, which is then compared with the wind loads to integrate the convolution integral and approximate the probability of failure of the system P_f or the reliability index β using MATLAB [55]. Instead of adopting the standard random sampling method, the implementation of the more efficient Latin-Hypercube sampling (LHS) technique allowed reducing the number of required simulations to typically 200 cases per frame and dead load case [14].

To complement the reliability calibrations of stainless steel frames under gravity loads carried out in [21], and since the design of steel portal frames is generally governed by load combinations that include wind loads, this study considered loading scenarios comprising combined dead and wind loads. According to [44], including live loads in reliability analyses has a negligible effect on the calibrated reliabilities except for those cases where nominal live-to-dead load ratios L_n/D_n are high and nominal wind-to-dead load ratios W_n/D_n are low, but in such cases gravity loads are found to govern the design of the frames. Furthermore, the frames considered in this study are often slab on grade, in which the live load is carried by the slab, and the roof live loads are not likely to be present in high wind speed ultimate limit state scenarios. The ultimate limit state load combinations for dead and wind loads according to the prEN 1990 [53], ASCE 7-16 [38] and AS/NZS 1170.0 [54] specifications are given by Eq. (9) to Eq. (11) for the Eurocode, US and Australian design frameworks, where G_k, D_n and G_n represent the characteristic (or nominal) dead loads and $W_{k,50}$ and $W_{n,i}$ correspond to the characteristic (or nominal) wind loads.

$$\text{Eurocode framework: } 1.35G_k + 1.5W_{k,50} \quad (9)$$

$$\text{US framework: } 1.20D_n + W_{n,700} \quad (10)$$

$$\text{Australian framework: } 1.20G_n + W_{n,500} \quad (11)$$

Nevertheless, the reliability of structural systems depends on the load ratios, obtaining different reliability index β values for varying live-to-dead load ratios [11,21] and for varying wind-to-gravity load ratios [11-14] since each loading type shows a different variability (see Table 2). To account for this effect, and in order to consider loading scenarios with different wind predominance, three different levels of design dead loads were considered in this study, defining load cases GW1, GW2 and GW3, which represent wind-to-dead load ratios ranging between 2.5 and 7. These dead loads corresponded to dead-to-total load ratios of 0.10–0.33, which are values commonly adopted in practice for portal frames under combined dead and wind load scenarios [14]. According to [56], low dead load ratios (or high wind-to-total load ratios) are aligned with the lowest reliability indices and thus, the safety or resistance factors calibrated using these load ratios correspond to the most unfavourable design situations. For each frame and each design dead load, five values of the system safety factor $\gamma_{M,s}$ (1.00, 1.05, 1.15, 1.25 and 1.55) and five values of the system resistance factor ϕ_s (0.75, 0.80, 0.85, 0.90 and 0.95) were considered to calibrate the associated system reliabilities. These values were chosen with the aim of obtaining a range of reliability indices β between 2.50 and 3.80 for the Eurocode framework and between 2.50 and 3.00 for the US/Australian frameworks. Note that although according to Table 2 the dead loads show a variability of 0.10, the numerical simulations carried out in this study treated the dead load as deterministic, for simplicity and following a similar approach to that adopted in [14]. A prior analysis on Frames 1 and 6 indicated that the impact of considering dead loads as random variables on the mean and COV values of the strength distribution is minimal, with the differences in the calibrated β-values being less than 1%. This is a result of the uncertainties associated with dead loads being significantly smaller than those of wind loads (see Table 2).

5. System strength calibration results

The results of the reliability calibrations carried out for stainless steel frames subjected to combined gravity and wind loads are presented and discussed in this Section. First, system strength distributions obtained for the six portal frames and the different dead load levels investigated are presented, and the reliability calibration results corresponding to the Eurocode, US and Australian frameworks are subsequently reported and compared. Then, suitable values for system safety factors $\gamma_{M,s}$ and system resistance factors ϕ_s are recommended for the direct design of stainless steel frames subjected to combined gravity and wind loads for different target reliability indices. Finally, the calibrated system safety

factors are compared with the values obtained from the semi-probabilistic approach detailed in prEN 1990 [53], and the solutions obtained using the *single-step* approach are compared with the stainless steel frames designed using the traditional *two-step* approach in terms of material consumption.

5.1. System strength of stainless steel frames under gravity and wind loads

System lateral strength R_w distributions for stainless steel frames subjected to combined gravity and wind loads were determined from extensive numerical simulations using the advanced FE models presented in Section 2, which accounted for all the relevant uncertainties according to the stochastic models described in Section 4.1. Ultimate frame loads were obtained from the load-lateral drift curves determined from finite element simulations for the apex joints. Following the approach adopted in previous studies [14,21,57], for frames showing load-lateral drift curves with a clearly defined peak point the ultimate load was adopted as this peak load. Conversely, for frames with no clear peak point in the load-lateral drift curves, the ultimate load was obtained as the load at which the stiffness of the curve fell below 5% of the

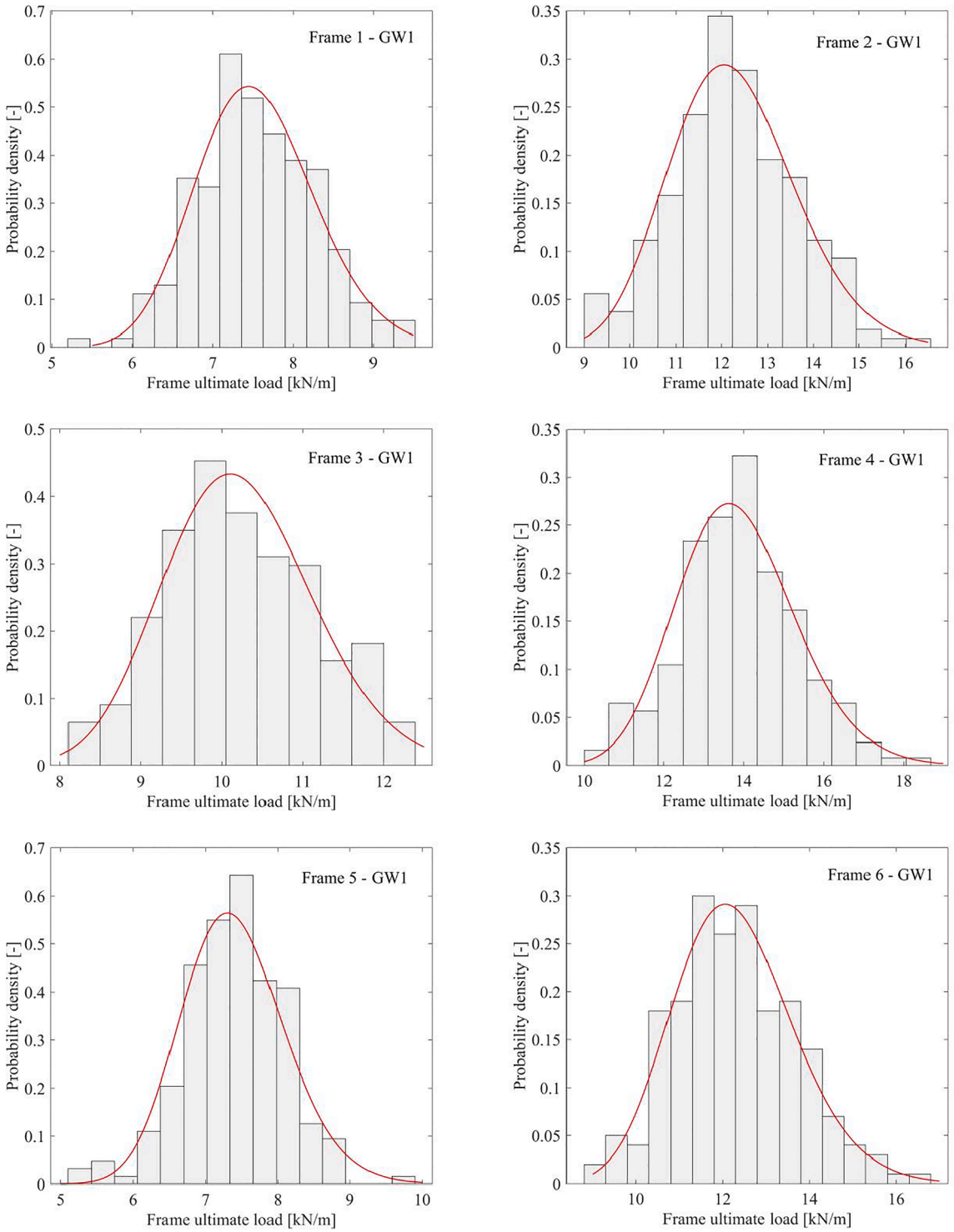

Fig. 4. Typical histograms for system lateral strength of stainless steel frames under the GW1 dead and wind load case for Frames 1 to 6.

initial stiffness. For the six stainless steel frames, histograms including the individual random system lateral strengths R_w were built for the different dead loads investigated (load cases GW1, GW2 and GW3), from which the different stochastic models for $R_{w,i}$ were determined. All system strength distributions were fitted by log-normal distributions using the Statistics and Machine Learning Toolbox in MATLAB [55] based on the maximum likelihood method, and the resulting distributions were evaluated using Anderson-Darling goodness-of-fit tests at the 5% significance level. It should be noted that the choice of a log-normal distribution to model frame strength histograms is consistent with the distributions adopted in previous studies for system strengths of steel and stainless steel structures [10,13,14,21]. Fig. 4 shows typical examples of the histograms obtained from the system lateral strengths and the fitted log-normal distributions corresponding to the six frames investigated for the load case GW1, representing the lowest wind-to-dead load ratio. It is worth noting that since the system lateral strength distributions were derived from numerical simulations based on probabilistic models for material, imperfection, geometric and connection characteristics calibrated from actual stainless steel structures, they can be used to carry out reliability calibrations in the three design frameworks considered in this study.

The mean values of the system lateral strengths $\overline{R}_w$ and corresponding coefficients of variation $V_{R,w}$ for the three dead load cases are reported in Table 4 for the six baseline frames. The results in Table 4 indicate that the mean system lateral strengths $\overline{R}_w$ increased as the dead loads applied decreased, since the design wind load became more dominant. The results also suggest that the uncertainty (i.e., $V_{R,w}$ values) of the system lateral strengths under different dead load levels were very similar for the six frames, but reduced slightly as the G_k or D_n values reduced. In general, comparable values of COV can be observed for all frames, lying between 0.090 and 0.113, although the lowest values of uncertainty were obtained for Frames 1, 3 and 5, which corresponded to frames with short spans and considerably stocky cross-sections. Among the different stainless steel families investigated, duplex alloys (Frames 3 and 4) were found to show the lowest $V_{R,w}$ values.

The values of the characteristic or nominal FE wind loads W_k or W_n associated with the different values of system safety factors $\gamma_{M,s}$ or system resistance factors ϕ_s for the Eurocode, US and Australian frameworks are presented in Table 5. Fifteen combinations of G_k and $\gamma_{M,s}$ (or D_n and ϕ_s) were investigated per design framework and for each frame, with a total of 45 cases per frame. Using the results in Table 4 and Table 5, the mean resistance-to-nominal wind ratios $\overline{R}_w/W_k$ and $\overline{R}_w/W_n$ were calculated for the six frames, and the average values corresponding to each dead load level (considering the different $\gamma_{M,s}$ and ϕ_s-factors analysed) are reported in the last columns of Table 4 for the three design frameworks. These ratios show a significant difference between the Eurocode and the US/Australian frameworks, with the $\overline{R}_w/W_k$ ratios calculated for the Eurocode being remarkably higher for all the frames. This is because the W_k and W_n values were determined such that the frames satisfied design equations Eq. (1) and Eq. (2), which depend on the load combination prescribed for each design framework. The prEN 1990 [53] load combination for wind loading given in Eq. (9) features a load factor $\gamma_W = 1.50$, while this factor is equal to 1.0 in the ASCE 7-16 [38] and AS/NZS 1170.0 [54] standards (see Eq. (10) and Eq. (11)) since the nominal loads in ASCE 7-16 and AS/NZS 1170.0 correspond to considerably higher return periods, as discussed in Section 4.2. With higher prescribed nominal wind loads W_n, the $\overline{R}_w/W_n$ ratios obtained for the US/Australian frameworks were lower than for the Eurocode.

Analysing the mean resistance-to-nominal wind ratios reported in Table 4 for the Eurocode framework it is evident that austenitic and ferritic stainless steel frames (Frames 1, 2, 5 and 6) showed similar strength reserves (i.e., $\overline{R}_w/W_k$ ratios) due to the equivalent overstrength ratios (i.e., mean-to-nominal yield stress ratios) exhibited by these materials. On the contrary, the values reported for duplex frames (Frames 3 and 4) are lower, owing to their lower overstrength ratio. The nominal wind load W_n values obtained for the US and Australian frameworks were very similar for all the frames investigated, because the load combinations (see Eq. (10) and Eq. (11)) and nominal FE models (material properties and imperfections) adopted in the two frameworks were almost identical. However, the relative comparison of the $\overline{R}_w/W_n$ ratios reported for the six stainless steel frames within the US or Australian frameworks shows that the lowest $\overline{R}_w/W_n$ ratios were observed for duplex frames (Frames 3 and 4), followed by ferritic frames (Frames 5 and 6) and austenitic frames (Frames 1 and 2). This can be explained by the considerably lower nominal material properties defined in the ASCE 8 [7] and AS/NZS 4673 [8] specifications for austenitic and duplex stainless steel alloys, which means that the overstrength ratios corresponding to the nominal ASCE 8 and AS/NZS 4673 material properties are significantly higher than the ratios obtained for the nominal properties prescribed in EN 10088-4 [26]. Overstrength ratios corresponding to the ASCE 8 [7] and AS/NZS 4673 [8] nominal material properties would be around 1.45, 1.25 and 1.30 for the ASTM 304, ASTM 2205 and ASTM UNS S40977 stainless steel grades, respectively, which align with the $\overline{R}_w/W_n$ ratios for the different materials. Similar observations were also reported for stainless steel frames under gravity loads in [21].

Table 4
Statistics of system lateral strength for stainless steel frames subjected to combined gravity and wind loads.

Frame	G_k, D_n or G_n [kN/m]	$\overline{R}_w$ [kN/m]	$V_{R,w}$	Eurocode framework $\overline{R}_w/W_k$	US framework $\overline{R}_w/W_n$	Australian framework $\overline{R}_w/W_n$
Frame 1	1.00	7.560	0.097	2.11	1.52	1.51
	0.75	7.584	0.097	2.08	1.50	1.50
	0.60	7.636	0.094	2.08	1.50	1.50
Frame 2	1.40	12.281	0.111	2.08	1.55	1.54
	1.20	12.368	0.110	2.08	1.55	1.54
	1.00	12.428	0.110	2.06	1.55	1.54
Frame 3	2.00	10.083	0.094	1.94	1.35	1.35
	1.50	10.154	0.093	1.92	1.34	1.34
	1.00	10.231	0.090	1.91	1.33	1.33
Frame 4	2.00	13.861	0.106	1.96	1.41	1.41
	1.60	13.898	0.104	1.90	1.37	1.37
	1.40	13.909	0.101	1.86	1.34	1.34
Frame 5	1.00	7.404	0.094	2.10	1.38	1.39
	0.75	7.452	0.093	2.08	1.37	1.38
	0.60	7.478	0.092	2.07	1.37	1.38
Frame 6	1.60	12.291	0.113	2.19	1.42	1.43
	1.40	12.355	0.113	2.16	1.41	1.42
	1.20	12.419	0.112	2.14	1.40	1.41

Table 5
Nominal system lateral strength for stainless steel frames subjected to combined gravity and wind loads for different system safety ($\gamma_{M,s}$) and resistance (ϕ_s) factors.

Design framework	Dead load case	$\gamma_{M,s}$ or ϕ_s	W_k or W_n [kN/m]					
			Frame 1	Frame 2	Frame 3	Frame 4	Frame 5	Frame 6
Eurocode framework	$G_{k,1}$	$\gamma_{M,s} = 1.00$	4.37	7.18	6.34	8.79	4.30	6.91
		$\gamma_{M,s} = 1.05$	4.14	6.84	6.02	8.32	4.07	6.53
		$\gamma_{M,s} = 1.15$	3.76	6.20	5.45	7.50	3.70	5.92
		$\gamma_{M,s} = 1.25$	3.44	5.66	5.00	6.78	3.39	5.40
		$\gamma_{M,s} = 1.55$	2.72	4.46	3.93	5.19	2.67	4.18
	$G_{k,2}$	$\gamma_{M,s} = 1.00$	4.41	7.24	6.41	9.00	4.35	6.97
		$\gamma_{M,s} = 1.05$	4.20	6.89	6.08	8.52	4.12	6.64
		$\gamma_{M,s} = 1.15$	3.82	6.25	5.53	7.74	3.76	6.01
		$\gamma_{M,s} = 1.25$	3.49	5.70	5.09	7.03	3.44	5.49
		$\gamma_{M,s} = 1.55$	2.79	4.53	4.05	5.46	2.75	4.29
	$G_{k,3}$	$\gamma_{M,s} = 1.00$	4.44	7.34	6.47	9.17	4.37	7.08
		$\gamma_{M,s} = 1.05$	4.22	6.94	6.14	8.68	4.16	6.69
		$\gamma_{M,s} = 1.15$	3.84	6.34	5.61	7.83	3.78	6.11
		$\gamma_{M,s} = 1.25$	3.53	5.79	5.14	7.16	3.48	5.57
		$\gamma_{M,s} = 1.55$	2.82	4.60	4.13	5.60	2.77	4.39
US framework	$D_{n,1}$	$\phi_s = 0.75$	4.41	6.99	6.58	8.56	4.74	7.60
		$\phi_s = 0.80$	4.70	7.53	7.04	9.26	5.08	8.17
		$\phi_s = 0.85$	5.03	8.00	7.51	9.98	5.40	8.75
		$\phi_s = 0.90$	5.35	8.47	8.01	10.64	5.75	9.33
		$\phi_s = 0.95$	5.65	9.01	8.46	11.30	6.06	9.93
	$D_{n,2}$	$\phi_s = 0.75$	4.46	7.06	6.70	8.92	4.81	7.72
		$\phi_s = 0.80$	4.78	7.53	7.15	9.58	5.13	8.30
		$\phi_s = 0.85$	5.08	8.06	7.63	10.25	5.48	8.88
		$\phi_s = 0.90$	5.38	8.54	8.10	10.93	5.81	9.41
		$\phi_s = 0.95$	5.68	9.01	8.55	11.61	6.13	10.01
	$D_{n,3}$	$\phi_s = 0.75$	4.51	7.12	6.80	9.11	4.84	7.84
		$\phi_s = 0.80$	4.81	7.59	7.26	9.78	5.19	8.43
		$\phi_s = 0.85$	5.11	8.06	7.71	10.46	5.51	8.95
		$\phi_s = 0.90$	5.44	8.61	8.20	11.14	5.84	9.55
		$\phi_s = 0.95$	5.75	9.09	8.65	11.76	6.16	10.08
Australian framework	$G_{n,1}$	$\phi_s = 0.75$	4.41	7.06	6.58	8.56	4.71	7.54
		$\phi_s = 0.80$	4.76	7.53	7.04	9.26	5.05	8.10
		$\phi_s = 0.85$	5.02	8.00	7.51	9.98	5.37	8.68
		$\phi_s = 0.90$	5.32	8.54	8.01	10.64	5.72	9.26
		$\phi_s = 0.95$	5.65	9.01	8.46	11.30	6.03	9.85
	$G_{n,2}$	$\phi_s = 0.75$	4.49	7.12	6.70	8.92	4.79	7.66
		$\phi_s = 0.80$	4.78	7.59	7.15	9.58	5.11	8.23
		$\phi_s = 0.85$	5.11	8.06	7.63	10.25	5.43	8.82
		$\phi_s = 0.90$	5.41	8.54	8.10	10.93	5.78	9.33
		$\phi_s = 0.95$	5.71	9.09	8.55	11.61	6.10	9.93
	$G_{n,3}$	$\phi_s = 0.75$	4.51	7.18	6.80	9.11	4.81	7.78
		$\phi_s = 0.80$	4.84	7.65	7.26	9.78	5.13	8.36
		$\phi_s = 0.85$	5.14	8.13	7.71	10.46	5.45	8.88
		$\phi_s = 0.90$	5.44	8.61	8.20	11.14	5.81	9.48
		$\phi_s = 0.95$	5.75	9.09	8.65	11.76	6.13	10.01

5.2. Reliability calibration results for frames under gravity and wind loads

System reliability indices β derived for stainless steel portal frames subjected to combined gravity and wind loads for a period of reference of 50 years are presented in this Section. The results were obtained following the methodology described in Section 4.3, the probabilistic models for system lateral resistance presented in Section 5.1 and the appropriate stochastic models for wind loads for the three design frameworks.

The system reliability indices β determined for the three dead load levels investigated for each stainless steel frame and the different values of system safety factor $\gamma_{M,s}$ or system resistance factors ϕ_s considered are presented in Fig. 5 for the Eurocode, US and Australian design frameworks as $\beta - \gamma_{M,s}$ and $\beta - \phi_s$ relationships. The results in Fig. 5 demonstrate that the reliability indices β increased with increasing system safety factors $\gamma_{M,s}$ but decreased with increasing system resistance factors ϕ_s, since the resistance factor can be considered equivalent to the inverse of the safety factor. The relative reliability indices obtained for the six stainless steel frames within each of the design frameworks were consistent with the mean resistance-to-nominal wind ratios $\overline{R}_w/W_k$ or $\overline{R}_w/W_n$ presented and discussed in Section 5.1 and with the overstrength ratios (i.e., mean-to-nominal yield stress ratios) characterizing each stainless steel family. The lowest reliability indices were observed for duplex frames (Frames 3 and 4), followed by ferritic (Frames 5 and 6) and austenitic frames (Frames 1 and 2). While the results for austenitic and ferritic frames were very similar in the Eurocode framework, owing to the same overstrength ratios exhibited by these materials, the reliability indices derived for austenitic frames in the US/Australian framework were remarkably higher. This is to be expected as the low nominal yield stress values prescribed in ASCE 8 [7] and AS/NZS 4673 [8] for the EN 1.4301/ASTM 304 grades resulted in higher mean-to-nominal resistance ratios than those observed for the Eurocode framework.

The differences in the reliability indices β shown in Fig. 5 among the three design frameworks investigated were in general smaller than those observed for the same frames under gravity loads only [21] for equivalent $\gamma_{M,s}$ or ϕ_s factors. This can be attributed to the similarities in the stochastic definition of the wind loads for the different design frameworks (see Table 2 for a return period of T = 50 years). Despite return

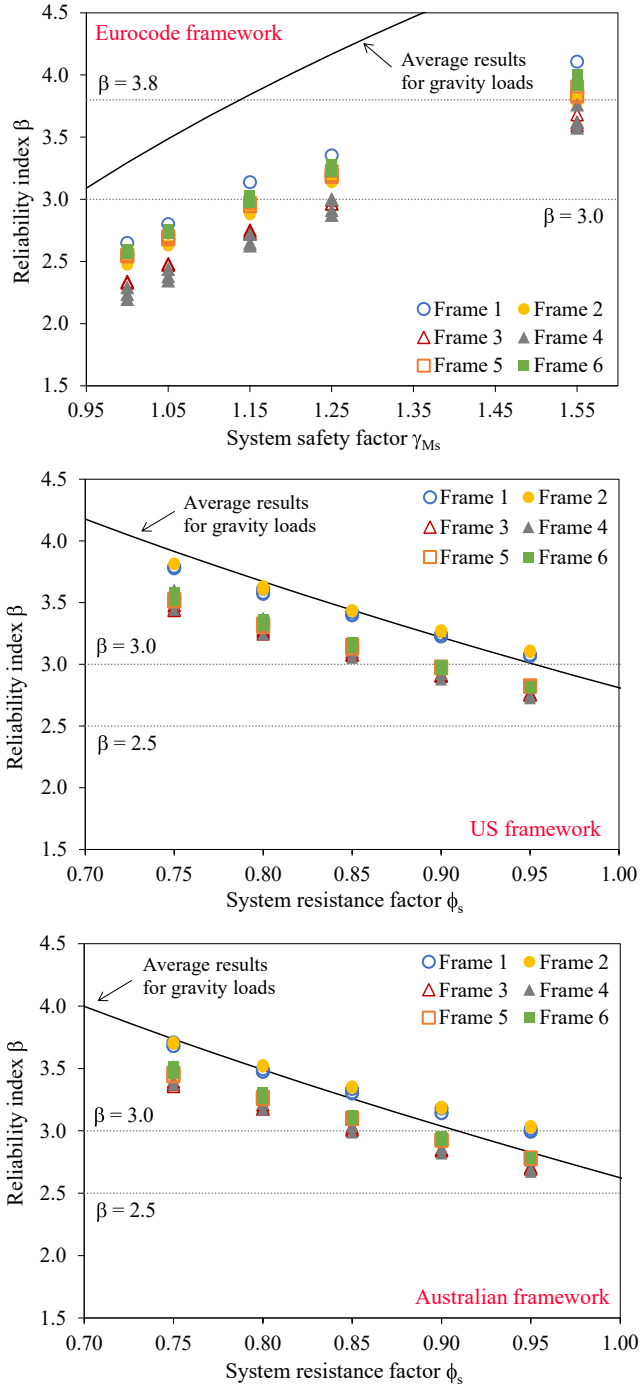

Fig. 5. Calibrated $\beta - \gamma_{M,s}$ and $\beta - \phi_s$ relationships for stainless steel frames subjected to combined gravity and wind loads for the Eurocode, US and Australian design frameworks.

periods used in the definition of the nominal wind loads in prEN 1991-1-4 [37], ASCE 7-16 [38] and AS/NZS 1170.2 [39] being different, as discussed in Section 4.2, it should be noted that the nominal wind loads in the wind-dominated load combinations prescribed in prEN 1990 [53], ASCE 7-16 [38] and AS/NZS 1170.0 [54], and shown in Eq. (9) to Eq. (11), are multiplied by different load factors: while the characteristic wind loads in the Eurocode are multiplied by a load factor of $\gamma_W = 1.50$, nominal wind loads adopt a load factor equal to unity in the US and Australian frameworks. Coefficients relating wind loads for a return period of T = 50 years and the nominal return periods in ASCE 7-16 [38] and AS/NZS 1170.2 [39] are, as calculated in Section 4.2, $W_{n,700}/W_{n,50} = 1.60$ and $W_{n,500}/W_{n,50} = 1.51$, respectively, which are similar to the $\gamma_W = 1.50$ factor adopted in the Eurocode. Hence, the final wind loads adopted for the reliability calibrations in the three design frameworks are comparable and produced similar values of reliability indices β.

Fig. 5 also shows the average $\beta - \gamma_{M,s}$ and $\beta - \phi_s$ curves derived in [21] for stainless steel frames under gravity loads only. The comparison of the reliability indices corresponding to gravity loads and to combined gravity and wind loads showed that differences exist in structural reliability for different load combinations; this is a well-known fact for the three design frameworks investigated [44,58-62]. This safety differentiation with respect to the type of loading was attributed to economic reasons and to the fact that the wind load models contained many conservative assumptions for the Eurocode [56,61,62]. Likewise, different authors have highlighted the fact that the reliability indices obtained for the US and Australian frameworks by calibration to existing and acceptable designs for wind is less than that for structures in which gravity loads govern [11,12,44,58,59].

5.3. Discussion and recommendations

This Section presents a discussion on the appropriate target reliability indices β_0 for structures dominated by wind loads and, based on these β_0-values, provides recommendations for the system safety factors $\gamma_{M,s}$ and resistance factors ϕ_s to be adopted in the direct design of stainless steel frames subjected to combinations of gravity and wind loads.

The minimum value of the target reliability index recommended in prEN 1990 [53] for ultimate limit states in RC2 reliability class structures and a 50-years reference period is $\beta_0 = 3.8$, which is commonly considered in the reliability analyses carried out for the Eurocode framework [19,41,61]. Although the reliability indices obtained for members through the traditional member-based design methodology are not directly comparable to those corresponding to system-based design approaches, and the β_0-values in prEN 1990 [53] generally correspond to member-based design, the same target value has been preliminarily adopted in this study. In statically determinate frames, or when failure occurs in a statically determinate part of a redundant frame, the target reliability of member-based and system-based approaches should be the same. In the case of statically redundant frames, where system-based methodologies account for the additional frame capacity arising from the load redistribution after the critical member reaches its capacity, the system target reliability index should be chosen to be at least that of the member-based methodology. Likewise, ASCE 7-16 [38] prescribes different target reliability indices depending on the Risk Category of the structure and the failure mode considered. For Risk Categories I and II structures showing failure modes that are not sudden and do not lead to wide-spread progression of damage, which is the case for the frames analysed in this paper, the prescribed target reliabilities are $\beta_0 = 2.5$ and $\beta_0 = 3.0$, respectively, for reference periods of 50 years. For non-ductile failure modes, including the failure of columns and connections, ASCE 7-16 requires higher target reliabilities.

Considering that Fig. 5 reports the reliability results for different wind-to-dead load ratios for each system safety factor $\gamma_{M,s}$ and system resistance factor ϕ_s considered, and that for a given safety or resistance factor the markers for the different wind-to-dead load ratios are hardly discernible, it can be concluded that the wind-to-dead load ratio has a negligible effect on the reliability index β. The required factors for achieving the target reliability indices are also not the same for the different frames. However, for design purposes a single value of $\gamma_{M,s}$ or ϕ_s is desirable and thus, average system reliabilities were considered in this study with the aim of recommending safety and resistance factors. Table 6 reports the average values of reliability indices β corresponding to the three levels of dead load for each baseline frame, a reference period of 50 years and different system safety factors $\gamma_{M,s}$ or system

Table 6
Summary of system reliability indices β of stainless steel frames subjected to combined gravity and wind loads (average of three dead load cases GW1, GW2 and GW3).

Design framework	$\gamma_{M,s}$ or ϕ_s	Frame 1	Frame 2	Frame 3	Frame 4	Frame 5	Frame 6	Average
Eurocode framework	$\gamma_{M,s} = 1.00$	2.58	2.49	2.33	2.24	2.55	2.59	2.46
	$\gamma_{M,s} = 1.05$	2.72	2.63	2.48	2.39	2.69	2.74	2.61
	$\gamma_{M,s} = 1.15$	3.01	2.89	2.74	2.67	2.95	3.00	2.88
	$\gamma_{M,s} = 1.25$	3.24	3.15	2.97	2.93	3.20	3.25	3.12
	$\gamma_{M,s} = 1.55$	3.94	3.80	3.63	3.65	3.86	3.95	3.81
US framework	$\phi_s = 0.75$	3.78	3.81	3.45	3.52	3.52	3.55	3.60
	$\phi_s = 0.80$	3.59	3.62	3.26	3.30	3.32	3.34	3.40
	$\phi_s = 0.85$	3.41	3.44	3.08	3.11	3.14	3.15	3.22
	$\phi_s = 0.90$	3.23	3.27	2.91	2.93	2.97	2.98	3.05
	$\phi_s = 0.95$	3.07	3.11	2.76	2.76	2.82	2.82	2.89
Australian framework	$\phi_s = 0.75$	3.69	3.70	3.37	3.43	3.41	3.43	3.51
	$\phi_s = 0.80$	3.48	3.52	3.19	3.23	3.26	3.28	3.33
	$\phi_s = 0.85$	3.32	3.35	3.02	3.04	3.10	3.11	3.15
	$\phi_s = 0.90$	3.11	3.19	2.85	2.87	2.93	2.89	2.97
	$\phi_s = 0.95$	3.00	3.03	2.70	2.71	2.72	2.75	2.82

resistance factors ϕ_s. Averaged values considering all frames are also provided for each $\gamma_{M,s}$ or ϕ_s-factor. Using the reliability indices presented in Table 6, it is possible to determine the required system safety factors $\gamma_{M,s}$ and system resistance factors ϕ_s for the target reliability indices associated with the different design frameworks, which are reported in Table 7. The $\gamma_{M,s}$ and ϕ_s values included in Table 7 were calculated using linear interpolation between the reliability indices β shown in Table 6 for each of the six frames and a range of target reliability indices β_0, from which the average values considering all frames were determined. It is worth noting that some of the $\gamma_{M,s}$-factors reported in Table 7 are below unity, while values above unity can be found for the US and Australian frameworks, particularly for the lowest β_0-values considered. This can be explained by the $\overline{R}_w/W_k$ and $\overline{R}_w/W_n$ ratios obtained for the investigated frames, which exhibited sufficient strength reserve to meet some of the lowest reliability requirements without needing additional system factors ($\gamma_{M,s}$ or ϕ_s) to be adopted.

Since the required system resistance factors ϕ_s to meet a target reliability index β_0 of 3.0 ranged between 0.87 and 0.98 for the different frames in the US framework, and between 0.85 and 0.96 in the Australian framework (see Table 7), with respective average values of 0.91 and 0.90, a ϕ_s-factor of 0.90 is recommended for the US and Australian frameworks for combined gravity and wind load cases. It is worth mentioning that for a similar target reliability index the ϕ_s-factors recommended in [21] for gravity loads only were 0.95 and 0.90 for the US and Australian frameworks, respectively. The ϕ_s-factors corresponding to a target value of about $\beta_0 = 2.50$ proposed in previous studies for steel frames subjected to combined gravity and wind loads in the US framework were $\phi_s = 0.80-0.85$ for hot-rolled planar frames [11], $\phi_s = 0.85$ for hot-rolled spatial frames [12], $\phi_s = 0.85-0.90$ for cold-formed spatial frames [13] and $\phi_s = 0.85$ for cold-formed portal frames with locally unstable members [14]. These values are more conservative than the ϕ_s-factors calibrated herein due to the higher mean-to-nominal resistance ratios obtained for stainless steel frames as a result of the higher mean-to-nominal yield stress ratios.

Similarly, the required system safety factors $\gamma_{M,s}$ for the target reliability index of $\beta_0 = 3.8$ prescribed in prEN 1990 [53] ranged between 1.48 and 1.63, with an average value of $\gamma_{M,s} = 1.55$, according to the values reported in Table 7. This is a significantly high safety factor compared to the $\gamma_{M0} = \gamma_{M1} = 1.10$ values recommended in the current prEN 1993-1-4 [5] standard for the traditional design of stainless steel cross-sections and members. It is also remarkably higher than the value recommended in [21] for gravity loads only, $\gamma_{M,s} = 1.15$. The high $\gamma_{M,s}$-values are due to the fact that the load factor prescribed for wind loads in the Eurocode is insufficient to guarantee the required level of reliability for reasonable values of partial safety factors; the need for load factors γ_W higher than the prescribed value of 1.50 for wind and snow loads in the Eurocode framework has been already highlighted in [49,60], which is equivalent to considering that the actual reliability index β_0 for wind loading is lower than 3.8. An estimation of the required γ_W-factor to achieve a β_0-value of 3.8 can be obtained from Eq. (12), which provides the relationship between the design load and the mean load for different fractile levels corresponding to failure probabilities of P_f for Gumbel distributions – note that $P_f = \Phi(-\beta)$ [49]. Considering that the load factor for wind is defined as $\gamma_W = W_d/W_k$ and that the mean-to-characteristic load ratio $\overline{W}/W_k$ is already known from Section 4.2, a relationship between γ_W and P_f (or β) can be derived. Using the sensitivity factor $\alpha_E = 0.7$ prescribed in the Eurocode for loads [53], the wind load factor required to meet a level of reliability of

Table 7
System safety factors $\gamma_{M,s}$ and system resistance factors ϕ_s for stainless steel frames subjected to combined gravity and wind loads for different target reliability indices β_0.

Design framework	Target reliability index	Frame 1	Frame 2	Frame 3	Frame 4	Frame 5	Frame 6	Average
Eurocode framework $\gamma_{M,s}$	$\beta_0 = 2.50$	0.97	0.95	1.03	1.07	0.96	0.95	0.99
	$\beta_0 = 2.75$	1.04	1.09	1.15	1.18	1.07	1.05	1.09
	$\beta_0 = 3.00$	1.14	1.18	1.26	1.28	1.16	1.15	1.20
	$\beta_0 = 3.80$	1.49	1.55	1.63	1.61	1.52	1.48	1.55
US framework ϕ_s	$\beta_0 = 2.50$	1.13	1.13	1.03	1.03	1.06	1.05	1.07
	$\beta_0 = 2.75$	1.05	1.06	0.94	0.94	0.97	0.97	0.99
	$\beta_0 = 3.00$	0.97	0.98	0.87	0.87	0.88	0.89	0.91
	$\beta_0 = 3.50$	0.82	0.83	0.74	0.75	0.75	0.76	0.78
Australian framework ϕ_s	$\beta_0 = 2.50$	1.19	1.12	1.00	1.01	1.00	1.03	1.06
	$\beta_0 = 2.75$	0.99	1.04	0.93	0.93	0.96	0.95	0.96
	$\beta_0 = 3.00$	0.94	0.96	0.85	0.86	0.89	0.90	0.90
	$\beta_0 = 3.50$	0.80	0.81	0.72	0.73	0.72	0.72	0.75

$\alpha_E \cdot \beta_0 = 0.7 \cdot 3.8 = 2.66$ is $\gamma_W = 1.73$, which is significantly higher than the 1.50 codified value.

$$W_d/\overline{W} = 1 - 0.45V_W - 0.78V_W \ln\left(-\ln\left(1 - P_f\right)\right) \quad (12)$$

In view of this, there are two possible alternatives to calibrate a system safety factor for gravity plus wind load cases: (i) recognizing that the $\gamma_W = 1.50$ value prescribed in prEN 1990 [53] is not sufficient to meet a target reliability of $\beta_0 = 3.8$, a new value of the γ_W-factor can be derived to ensure that the required reliability criteria is met, which is the approach followed by Botha et al. [49] for the South African specification; or (ii) acknowledge that the level of reliability achieved for wind loads using a γ_W-factor of 1.50 is lower than that for gravity load scenarios and insufficient to guarantee the target reliability requirements [49,60], and thus to adopt a reduced target reliability to calibrate a system safety factor that is not too severe to achieve the full potential of system-based design approaches [63]. In this paper the second alternative was adopted in order to affect the design framework that is familiar to practicing engineers as little as possible, since while load factors are well-assimilated by designers, it is common to adopt a range of partial safety factors when working with different materials or failure modes. A reasonable reduced value for the target reliability index would be that adopted for the US and Australian design frameworks for wind load dominated structures, i.e., $\beta_0 = 3.0$. In this case, and according to the values reported in Table 7, the required $\gamma_{M,s}$-factors range between 1.14 and 1.28, with an average value of 1.20. Hence, a system safety factor of $\gamma_{M,s} = 1.20$ is recommended for stainless steel frames under gravity plus wind load cases.

5.4. Calibration using the Eurocode semi-probabilistic approach

To calibrate the $\gamma_{M,s}$-factor using the standard semi-probabilistic method given in prEN 1990 [53] Eq. (13) should be used, in which the $R_k/\overline{R}_w$-ratio accounts for the bias in the strength function. Considering that the average $R_k/\overline{R}_w$-ratio for the different frames is 1.13, that the sensitivity factor prescribed in the Eurocode is $\alpha_R = 0.8$ for resistance [53], and adopting a target reliability index of $\beta_0 = 3.8$, the average estimated system safety factor is $\gamma_{M,s} = 1.41$, different from the $\gamma_{M,s} = 1.55$ value calibrated in Section 5.2 for the same target reliability. This is because, as highlighted above, the actual level of reliability obtained for a load factor of $\gamma_W = 1.50$ is lower than the target value of 3.8. If the actual β (or P_f) is back-calculated from Eq. (12) for the wind load model adopted in this study, one obtains a reliability index of 3.2. The system safety factor resulting from Eq. (13) for this value of β is $\gamma_{M,s} = 1.15$, which differs by 10% from the value derived using the results in Table 6 for a corresponding value of $\beta_0 = 3.2$, $\gamma_{M,s} = 1.27$, in line with the findings reported in [64].

$$\gamma_{M,s} = (R_k/\overline{R}_w)\exp(\alpha_R \beta_0 V_{R,w}) \quad (13)$$

An alternative procedure would have been to re-run the reliability analyses described in Section 5.2 for the $\gamma_W = 1.73$ value derived in the previous Section, and to use the resulting values to calibrate the system safety factor $\gamma_{M,s}$ for a target reliability index of $\beta_0 = 3.8$. Since the use of $\gamma_W = 1.73$ would result in higher reliability indices than those reported in Table 6, the required $\gamma_{M,s}$-factor would be lower than the 1.55 value shown in Table 7 and comparable to the $\gamma_{M,s} = 1.41$ value obtained at the beginning of this Section.

5.5. Comparison with traditional two-step design solutions

In order to quantify the differences between stainless steel frames designed using the *single-step* direct approach developed in this paper and the traditional *two-step* approach in terms of material consumption, the different frames were re-designed using the provisions given in prEN 1993-1-4 [5], ASCE 8 [7] and AS/NZS 4673 [8]. For this comparison, the design loads W_{Ed} for each frame were defined as the ultimate nominal lateral strengths of the frames divided or multiplied by the $\gamma_{M,s}$ and ϕ_s-factors recommended in this paper (i.e., $W_{Ed} = W_k/\gamma_{M,s}$ and $W_{Ed} = \phi_s \cdot W_n$). Hence, it was assumed that the six baseline frames were precisely at their ultimate limit states under the design loads W_{Ed}, and the cross-section dimensions required to withstand these loads were determined using the *two-step* approach. The final designs corresponding to the traditional *two-step* approach are reported in Table 8. Note that the differences between the two design approaches would be larger in practice, since in this comparison only the strictly minimum section increases were determined with the aim of identifying the gains directly attributable to the use of the direct design approach, resulting in non-commercial cross-section shapes and thickness values, as indicated in Table 8.

According to these results, the frames designed using the traditional *two-step* approach required 14.3%, 16.1% and 15.6% more material consumption, on average, than the direct design approach for the Eurocode, US and Australian design frameworks, respectively. The differences are larger for the US and Australian frameworks because for these frameworks the recommended system ϕ_s-factors are equal to those codified in the codes for beams and columns (ϕ_c and ϕ_b) in [7,8], while the partial safety factor proposed for systems $\gamma_{M,s}$ in this paper is more conservative than the $\gamma_{M,0}$ and $\gamma_{M,1}$ values given in prEN 1993-1-4 [5]. It is also worth mentioning that, due to the low compression forces occurring in the columns for the investigated frames, the limiting strength check in all cases was the bending moment resistance of the critical cross-sections. The design equations for bending moment strength prescribed in prEN 1993-1-4 [5], ASCE 8 [7] and AS/NZS 4673 [8] tend to estimate the capacity of cross-sections better than the strength of members, and hence it is expected that the differences in material consumption between the two design approaches may be higher for structures showing member failure modes.

5.6. Recommendations for specification committees

Based on the results presented in this paper and the equivalent study for stainless steel frames under gravity loads reported in [21], two different sets of recommendations exist for each design framework in terms of system safety and resistance factors. Prescribing resistance factors that depend on the load combination would be, however, impractical from an implementation point of view. Considering the system factors calibrated for the two load combinations, it is preliminarily recommended to adopt the values derived in this paper for gravity plus wind load cases for all load combinations. Although these $\gamma_{M,s}$ and ϕ_s values might be too conservative for gravity load cases, the practical consequences of this decision are not expected to be too significant since the design of portal frames is generally governed by wind loads [14]. Moreover, the system factors for gravity loads calibrated in [21] correspond to dead and live (imposed) loads only, and do not consider other types of loads (i.e., snow loads) that exhibit greater variability, which would potentially result in $\gamma_{M,s}$ and ϕ_s-factors more similar to those derived in this paper. Nevertheless, and considering that the choice of target reliability indices ultimately rests with specification committees which may decide to require different target reliabilities for the ultimate limit state of systems and for members, as the consequences of the collapse of a system may be more severe than those of the failure of an individual member [63], Table 7 also reports system safety factors $\gamma_{M,s}$ and system resistance factors ϕ_s for a range of β_0 values.

The $\gamma_{M,s}$ and ϕ_s factors recommended in this paper for stainless steel frames under combined gravity and wind loads, and in [21] for gravity loads, are calibrated for the ultimate limit state check. However, stainless steels exhibit a pronounced nonlinear stress *vs* strain behaviour with a gradual loss of stiffness even for low values of strain and consequently, serviceability limit states require greater attention than for steel structures. Independent reliability calibrations are thus necessary for

Table 8
Comparison between the required cross-section dimensions for the direct design and the *two-step* design approaches for different design frameworks.

Frame	Direct design approach	*Two-step* approach					
		Eurocode framework		US framework		Australian framework	
	Cross-section	Cross-section	Difference in area [%]	Cross-section	Difference in area [%]	Cross-section	Difference in area [%]
Frame 1	150×100×4	160×110×4.5	17.5	175×115×4.2	18.3	185×120×4.1	20.7
Frame 2	250×150×4	260×150×4.5	13.0	255×165×4.7	18.6	250×165×4.6	15.9
Frame 3	150×100×4	155×105×4.3	10.4	175×105×4.0	11.2	175×105×4.0	11.2
Frame 4	250×150×4	250×150×4.6	12.6	255×150×4.7	15.5	250×155×4.7	15.5
Frame 5	150×100×4	160×110×4.3	13.9	170×115×4.2	16.8	170×115×4.2	16.8
Frame 6	250×150×4	265×170×4.5	18.2	260×150×4.6	15.9	240×155×4.7	13.3
Average			14.3		16.1		15.6

serviceability, which are currently underway.

6. Conclusions

The latest versions of the main international design codes for steel and stainless steel structures [1-4] provide a basis for system-based design strategies by incorporating preliminary provisions of system-based direct design approaches. These approaches represent a change in the paradigm of structural design and will constitute the next generation of structural design standards, simplifying the design process and potentially leading to more efficient and lighter structures. Recommendations for the use of advanced direct design methods for steel structures have been already developed for different steel structures, including hot-rolled frames, cold-formed frames, racks and scaffolding structures. This study is part of a research effort to extend system-based direct design methods to stainless steel structures. The reliability framework for the design of stainless steel frames using advanced nonlinear numerical simulations was developed in [21,22], and was used in this paper. While [21] primarily focused on gravity loads, this study presents the system reliability calibrations for stainless steel portal frames subjected to combined gravity and wind loads.

The system reliability calibrations presented in this paper are based on extensive finite element simulations of six stainless steel portal frames covering austenitic, duplex and ferritic stainless steel alloys, which accounted for the effect of uncertainties in geometric properties, imperfections, residual stresses, material properties, connection stiffness and model uncertainty. The results showed that system reliability indices β derived for the European, US and Australian design frameworks for a reference period of 50 years were similar and consistent for the three frameworks, but lower than those derived under gravity loads [21]. Thus, different and slightly more conservative system factors $\gamma_{M,s}$ and ϕ_s were recommended for wind-dominated load cases. The results suggested that a system safety factor of $\gamma_{M,s} = 1.20$ is appropriate for the Eurocode framework to achieve a reduced target reliability index of $\beta_0 = 3.0$, while a resistance factor of $\phi_s = 0.90$ may be adopted for the US and Australian frameworks for a target reliability index of $\beta_0 = 3.0$. Since the choice of target reliability indices ultimately rests with specification committees, the tabulated values of system factors $\gamma_{M,s}$ and ϕ_s for a range of target reliability index values β_0 reported in this paper can be of assistance to these committees in choosing suitable values of $\gamma_{M,s}$ and ϕ_s corresponding to selected β_0-values.

Declaration of Competing Interest

The authors declare that they have no known competing financial interests or personal relationships that could have appeared to influence the work reported in this paper.

Acknowledgements

The project leading to this research has received funding from the European Union's Horizon 2020 Research and Innovation Programme under the Marie Sklodowska-Curie Grant Agreement No. 84239.

References

[1] AS/NZS 4100 Steel Structures. Standards Australia, Sydney, Australia; 2020.
[2] American Institute of Steel Construction (ANSI/AISC). AISC 360. Specification for Structural Steel Buildings. Illinois, USA; 2016.
[3] American Institute of Steel Construction (ANSI/AISC). AISC 370. Specification for Structural Stainless Steel Buildings. Illinois, USA; 2021.
[4] Working Group 22 for Eurocode 3, CEN/TC 250/SC3/WG22. prEN 1993-1-14. Eurocode 3: Design of steel structures – Part 1-14: Design assisted by finite element analysis. Brussels, Belgium. *Under development*.
[5] European Committee for Standardization (CEN). prEN 1993-1-4. Eurocode 3: Design of Steel Structures – Part 1-4: General Rules. Supplementary Rules for Stainless Steels. Final Document. Brussels, Belgium; 2021.
[6] European Committee for Standardization (CEN). prEN 1993-1-1. Eurocode 3: Design of Steel Structures – Part 1-1: General Rules and Rules for Buildings. Final Document. Brussels, Belgium; 2019.
[7] American Society of Civil Engineers (ASCE). SEI/ASCE 8. Specification for the Design of Cold-Formed Stainless Steel Structural Members. Virginia, USA; 2021.
[8] AS/NZS 4673 Cold-formed stainless steel structures. Standards Australia, Sydney, Australia; 2001.
[9] Zhang H, Liu H, Ellingwood BR, Rasmussen KJR. System reliabilities of planar gravity steel frames designed by the inelastic method in AISC 360–10. J. Struct. Eng. (ASCE) 2018;144(3):04018011.
[10] Zhang H, Shayan S, Rasmussen KJR, Ellingwood BR. System-based design of planar steel frames, I: Reliability framework. J Constr Steel Res 2016;123:135–43.
[11] Zhang H, Shayan S, Rasmussen KJR, Ellingwood BR. System-based design of planar steel frames, II: Reliability results and design recommendations. J Constr Steel Res 2016;123:154–61.
[12] Liu W, Zhang H, Rasmussen KJR, Yan S. System-based limit state design criterion for 3D steel frames under wind loads. J Constr Steel Res 2019;157:440–9.
[13] Liu W, Zhang H, Rasmussen KJR. System reliability-based Direct Design Method for space frames with cold-formed steel hollow sections. Eng Struct 2018;166:79–92.
[14] Sena Cardoso F, Zhang H, Rasmussen KJR, Yan S. Reliability calibrations for the design of cold-formed steel portal frames by advanced analysis. Eng Struct 2019;182:164–71.
[15] Sena Cardoso F, Zhang H, Rasmussen KJR. System reliability-based criteria for the design of steel storage rack frames by advanced analysis: Part II – Reliability analysis and design applications. Thin-Walled Struct 2019;141:725–39.
[16] Wang C, Zhang H, Rasmussen KJR, Reynolds J, Yan S. Reliability-based limit state design of support scaffolding systems. Eng Struct 2020;216:110677.
[17] Baddoo NR. Stainless steel in construction: A review of research, applications, challenges and opportunities. J Constr Steel Res 2008;64(11):1199–206.
[18] Gardner L. Stability and design of stainless steel structures – Review and outlook. Thin-Walled Struct 2019;141:208–16.
[19] Afshan S, Francis P, Baddoo NR, Gardner L. Reliability analysis of structural stainless steel design provisions. J Constr Steel Res 2015;114:293–304.
[20] NewGeneSS, New Generation Design Methods for Stainless Steel Structures. Marie Sklodowska-Curie Fellowship 2018, funded by the European Union's Horizon 2020 Research and Innovation Programme under Grant Agreement No. 842395.
[21] Arrayago I, Rasmussen KJR. System-based reliability analysis of stainless steel frames under gravity loads. Eng Struct 2021;231:111775. https://doi.org/10.1016/j.engstruct.2020.111775.
[22] Arrayago I, Rasmussen KJR, Real E. Statistical analysis of the material, geometrical and imperfection characteristics of structural stainless steels and members. J Constr Steel Res 2020;175:106378. https://doi.org/10.1016/j.jcsr.2020.106378.
[23] Arrayago I, Real E, Gardner L. Description of stress-strain curves for stainless steel alloys. Mater Des 2015;87:540–52.
[24] Rasmussen KJR. Full-range stress-strain curves for stainless steel alloys. J. Construct. Steel Res 2003;59(1):47–61.
[25] Steel Construction Institute (SCI). Design Manual for Structural Stainless Steel. Fourth Edition. UK; 2017.
[26] European Committee for Standardization (CEN). EN 10088-4. Stainless Steels Part 4: Technical Delivery Conditions for Sheet/Plate and Strip of Corrosion Resisting Steels for Construction Purposes. Brussels, Belgium; 2009.

[27] Rossi B, Afshan S, Gardner L. Strength enhancements in cold-formed structural sections – Part II: Predictive models. J Constr Steel Res 2013;83:189–96.
[28] Packer JA, Wardenier J, Kurobane Y, Dutta D, Yeomans N. Design guide for rectangular hollow section (RHS) joints under predominantly static loading. CIDECT Design Guide No, 3. Köln, Germany: Verlag TÜV Rheinland GmbH; 1992.
[29] ABAQUS. Version 6.10. Simulia, Dassault Systèmes, France; 2010.
[30] Arrayago I, Picci F, Mirambell E, Real E. Interaction of bending and axial load for ferritic stainless steel RHS columns. Thin-Walled Structures 2015;91:96–107.
[31] Becque J, Rasmussen KJR. A numerical investigation of local-overall interaction buckling of stainless steel lipped channel columns. J Constr Steel Res 2009;65(8-9):1685–93.
[32] Arrayago I, González-de-León I, Real E, Mirambell E. Tests on stainless steel frames. Part II: Results and analysis. Thin-Walled Structures 2020;157:107006. https://doi.org/10.1016/j.tws.2020.107006.
[33] Gardner L, Nethercot DA. Numerical modelling of stainless steel structural components – A consistent approach. J Struct Eng (ASCE) 2004;130(10):1586–601.
[34] Gardner L, Cruise RB. Modeling of residual stresses in structural stainless steel sections. J Struct Eng (ASCE) 2009;135(1):42–53.
[35] Olsson A. Constitutive modelling of stainless steel. J Constr Steel Res 1998;46(1-3):457. https://doi.org/10.1016/S0143-974X(98)80084-9.
[36] Arrayago I, González-de-León I, Real E, Mirambell E. Tests on stainless steel frames. Part I: Preliminary tests and experimental set-up. Thin-Walled Struct 2020;157:107005. https://doi.org/10.1016/j.tws.2020.107005.
[37] European Committee for Standardization (CEN). prEN 1991-1-4. Eurocode 1: Actions on structures – Part 1-4: Wind Actions. Final Document. Brussels, Belgium; 2019.
[38] American Society of Civil Engineers (ASCE). ASCE 7. Minimum design loads and associated criteria for buildings and other structures. Virginia, USA; 2016.
[39] AS/NZS, 1170.2 Structural design actions, Part 2: Wind actions 2011 Standards Australia, Sydney, Australia.
[40] Kwon DK, Kareem A. Comparative study of major international wind codes and standards for wind effects on tall buildings. Eng Struct 2013;51:23–35.
[41] Taras A, Huemer S. On the influence of the load sequence on the structural reliability of steel members and frames. Structures 2015;4:91–104.
[42] Gulvanessian H, Holicky M. Eurocodes: using reliability analysis to combine action effects. Proceed Institut Civil Eng - Struct Build 2005;158(4):243–52.
[43] Joint Committee on Structural Safety (JCSS). Probabilistic Model Code. Zurich, Switzerland; 2001.
[44] Ellingwood BR, Tekie PB. Wind load statistics for probability-based structural design. J Struct Eng (ASCE) 1999;125(4):453–63.
[45] McAllister TP, Wang N, Ellingwood BR. Risk-informed mean recurrence intervals for updated wind maps in ASCE 7–16. J Struct Eng (ASCE) 2018;144(5):06018001. https://doi.org/10.1061/(ASCE)ST.1943-541X.0002011.
[46] Ellingwood BR, Galambos TV, MacGregor JG, Cornell CA. Development of a Probability Based Load Criterion for American National Standard A58. Washington D.C: National Bureau of Standards. Special Publication No. 577; 1980.
[47] Holmes JD, Kwok KCS, Ginger JD. Wind loading handbook for Australia and New Zealand-background to AS/NZS 1170.2 wind actions. Report No. AWES-HB-001-2012. Australian Wind Engineering Society; 2012.
[48] Botha J, Retief JV, Viljoen C. Uncertainties in the South African wind load design formulation. J South Afr Institut Civil Eng 2018;60(3):16–29.
[49] Botha J, Retief JV, Viljoen C. Reliability assessment of the South African wind load design formulation. J South Afr Institut Civil Eng 2018;60(3):30–40.
[50] Holický M. Reliability Analysis for Structural Design. Stellenbosch: SUN MeDIA, ISBN 978-1-920338-11-4; 2009.
[51] Holický M, Marková J. Reliability of Concrete Elements Designed for Alternative Load Combinations Provided in Eurocodes. Acta Polytechnica 2003;43(1):29–33.
[52] Development of skills facilitating implementation of Eurocodes. Handbook 2: Reliability Backgrounds. Leonardo da Vinci pilot project CZ/02/B/F/PP-134007; 2005.
[53] European Committee for Standardization (CEN). prEN 1990. Eurocode: Basis of Structural Design. Draft Document. Brussels, Belgium; 2020.
[54] AS/NZS, 1170.0 Structural design actions, Part 0: General principles 2002 Standards Australia, Sydney, Australia.
[55] MATLAB version 9.8.0 (R2020a) The MathWorks Inc 2020 Natick, Massachusetts.
[56] Meinen NE, Steenbergen RDJM. Reliability levels obtained by Eurocode partial factor design - A discussion on current and future reliability levels. HERON 2018;63(3):243–302.
[57] Ziemian RD, McGuire W, Deierlein GG. Inelastic limit states design. Part I: planar frame studies. J Struct Eng (ASCE) 1992;118(9):2532–49.
[58] Ellingwood BR. LRFD: implementing structural reliability in professional practice. Eng Struct 2000;22(2):106–15.
[59] Ellingwood BR. Probability-based codified design: past accomplishments and future challenges. Struct Saf 1994;13(3):159–76.
[60] Joint Committee on Structural Safety (JCSS). Background Documentation Eurocode 1 (ENV 1991), Part 1: Basis of Design. ECCS Report No. 94; 1996.
[61] Steenbergen RDJM, Vrouwenvelder ACWM. Safety philosophy for existing structures and partial factors for traffic loads on bridges. HERON 2010;55(2):123–40.
[62] Vrouwenvelder ACWM, ScholtenNPM. Veiligheidsbeoordeling bestaande bouw, Achtergrondrapport bij NEN 8700 TNO Report 2008-D-R0015; 2008.
[63] Zhang H, Ellingwood BR, Rasmussen KJR. System reliabilities in steel structural frame design by inelastic analysis. Eng Struct 2014;81:341–8.
[64] Arrayago I, Zhang H, Rasmussen KJR. Simplified expressions for reliability assessments in code calibration. Eng Struct 2022;256:114013. https://doi.org/10.1016/j.engstruct.2022.114013.